

Article

## Carapanolides J–L from the Seeds of *Carapa guianensis* (Andiroba) and Their Effects on LPS-Activated NO Production

Yuuki Matsui <sup>1</sup>, Takashi Kikuchi <sup>1</sup>, Takanobu Inoue <sup>1</sup>, Osamu Muraoka <sup>2</sup>, Takeshi Yamada <sup>1</sup> and Reiko Tanaka <sup>1,\*</sup>

<sup>1</sup> Laboratory of Medicinal Chemistry, Osaka University of Pharmaceutical Sciences, 4-20-1 Nasahara, Takatsuki, Osaka 569-1094, Japan

<sup>2</sup> Faculty of Pharmaceutical Sciences, Kinki University, 3-4-1 Kowakae, Higashiosaka, Osaka 577-8502, Japan

\* Author to whom correspondence should be addressed; E-Mail: tanakar@gly.oups.ac.jp; Tel./Fax: +81-72-690-1084.

External Editor: Isabel C. F. R. Ferreira

Received: 5 September 2014; in revised form: 17 October 2014 / Accepted: 20 October 2014 /

Published: 24 October 2014

**Abstract:** A novel gedunin and two novel phragmalin-type limonoids, named carapanolides J–L (compounds **1–3**) as well as a known gedunin-type limonoid **4** were isolated from the seeds of *Carapa guianensis* (andiroba). Their structures were determined on the basis of 1D and 2D NMR spectroscopy and HRFABMS. Compounds **1–4** were evaluated for their effects on the production of NO in LPS-activated mouse peritoneal macrophages.

**Keywords:** *Carapa guianensis*; andiroba; seeds; gedunin; phragmalin; limonoids; NO production

### 1. Introduction

*Carapa guianensis* Aublet (Meliaceae), known locally as andiroba, is widely distributed in the Amazonas State of Brazil and its wood is extensively used as commercial timber [1]. Andiroba is a tall rainforest tree that grows up to 40 m in height. The indigenous people in the Amazon have used andiroba in many ways for centuries, and virtually all parts of the tree, as well as the seed oil, are utilized. It can be found growing wild throughout the Amazon rainforest, typically on rich soils, in swamps, and also in

the alluvial flats, marshes, and uplands of the Amazon Basin. This tree can also be found wild or under cultivation in Brazil in the Islands region, Tocantins, Rio Solimoes, and near the seaside. It is one of the large-leaved trees of the rainforest and can be identified by its large and distinctively textured leaves. The andiroba tree produces a brown, woody, four-cornered nut with a diameter of 3–4 inches that resembles a chestnut. Andiroba oil is a rich source of essential fatty acids including oleic, palmitic, stearic, and linoleic acids. It yields up to 65% unsaturated fatty acids and can contain approximately 9% linoleic acid. Andiroba oil extracts yield up to 65% unsaturated fatty acids and can contain approximately 9% linoleic acid. Extracts from its bark, flowers, and seeds have been used for centuries by the Amazonian people and exhibit various repellent [2], analgesic [3], anti-malarial [4], anti-inflammatory [5], anti-allergic [6], and antiplasmoidal [7] activities, as well as acute and subacute toxicities [8]. Our recent study on the components of the seed oil of *Carapa guianensis* revealed the structures of two new unusual 9,10-seco-mexicanolide-type limonoids, named carapanolides A and B [9], two novel carbon skeletal limonoids, named guianolides A and B [10], and carapanolides C–I [11]. We herein describe the isolation and structural determination of three novel limonoids **1–3**, named carapanolides J–L, and the effects of **1–3** and epoxyazadiradione (**4**) on the production of NO in LPS-activated mouse peritoneal macrophages. The structures of **1–3** were determined on the basis of NMR spectroscopy, including 1D and 2D (<sup>1</sup>H, <sup>1</sup>H-COSY, NOESY, HSQC, HMBC) NMR, and FABMS.

## 2. Results and Discussion

The seed oil of *Carapa guianensis* (2.03 kg) was separated by silica gel column chromatography, medium-pressure liquid chromatography (MPLC), and reverse-phase HPLC to obtain three new limonoids **1–3** and a known limonoid **4**, which was identified as epoxyazadiradione (Figure 1) [12].

The molecular formula of carapanolide J (**1**) was determined as C<sub>26</sub>H<sub>30</sub>O<sub>7</sub> ([M + H]<sup>+</sup> *m/z* 455.2075) based on HRFABMS. The IR and UV spectra showed bands assignable to a hydroxy group ( $\nu_{\text{max}}$  3503 cm<sup>-1</sup>), a six-membered ring ketone ( $\nu_{\text{max}}$  1727 cm<sup>-1</sup>), and an  $\alpha,\beta$ -unsaturated six-membered ring ketone [ $\nu_{\text{max}}$  1671 cm<sup>-1</sup>;  $\lambda_{\text{max}}$  230 nm (log ε 3.85)]. The <sup>1</sup>H and <sup>13</sup>C NMR spectra (Table 1) exhibited signals assignable to five tertiary methyls [ $\delta_{\text{H}}$  1.16, 1.17, 1.21, 1.28, and 1.56]; two CH<sub>2</sub> groups; five *sp*<sup>3</sup> methine groups, including three oxymethine [ $\delta_{\text{H}}$  3.88 (s), 4.47 (ddd), and 5.49 (s)]; five *sp*<sup>3</sup> quaternary carbons, including an oxycarbon [ $\delta_{\text{C}}$  65.4 (s)]; an  $\alpha,\beta$ -unsaturated six-membered ring ketone [ $\delta_{\text{H}}$  5.84, 8.24 (each 1H, d);  $\delta_{\text{C}}$  203.0 (s)]; a saturated ketone [ $\delta_{\text{C}}$  207.7 (s)]; δ-lactone [ $\delta_{\text{H}}$  5.49 (s);  $\delta_{\text{C}}$  166.4 (s)]; and furan ring [ $\delta_{\text{H}}$  6.39 (dd), 7.42 (t), 7.44 (m)]. In the HMBC spectrum, long-range correlations were observed between Me-18 ( $\delta_{\text{H}}$  1.21) and C-12, C-13, C-14 [ $\delta_{\text{C}}$  65.4 (s)], and C-17 [ $\delta_{\text{C}}$  77.6 (d)]; between Me-19 ( $\delta_{\text{H}}$  1.56) and C-1 ( $\delta_{\text{C}}$  160.2), C-5, C-9, and C-10; between Me-28 ( $\delta_{\text{H}}$  1.17) and C-3 ( $\delta_{\text{C}}$  203.0), C-4, C-5, and C-29; between Me-29 ( $\delta_{\text{H}}$  1.16) and C-3, C-4, C-5, and C-28; between Me-30 ( $\delta_{\text{H}}$  1.28) and C-7 ( $\delta_{\text{C}}$  207.7), C-8, C-9, and C-14; between H-11 ( $\delta_{\text{H}}$  4.47) and C-8, C-9, C-10, C-12, and C-13; between H-15 ( $\delta_{\text{H}}$  3.88) and C-8, C-13, C-14 and C-16 ( $\delta_{\text{C}}$  166.4); and between H-17 ( $\delta_{\text{H}}$  5.49) and C-12, C-13, C-14, C-16, C-18, C-20 [ $\delta_{\text{C}}$  120.0 (s)], C-21 [ $\delta_{\text{C}}$  141.1 (d)], and C-22 [ $\delta_{\text{C}}$  109.7 (s)] (Figure 2). An analysis of the <sup>1</sup>H-<sup>1</sup>H COSY spectrum (H-1–H-2; H-5–H<sub>2</sub>-6; H-9–H-11–H<sub>2</sub>-12; and H-22–H-23) revealed the partial structure shown in Figure 2. The HMBC and <sup>1</sup>H-<sup>1</sup>H COSY spectra revealed that **1** was a 11-hydroxy-7-deacetoxy-7-oxogedunin [13]. Selected NOESY correlations were shown in Figure 2. The secondary hydroxyl group at C-11 [ $\delta_{\text{H}}$  4.47 (ddd)] was determined to have an  $\alpha$  (equatorial)

orientation because significant NOEs were observed between H-11 and Me-19, and Me-30, while coupling constants were observed between H-11 $\beta$  and H-9 $\alpha$  ( $J_{11\beta,9\alpha} = 10.2$  Hz); H-11 $\beta$  and H-12 $\alpha$  ( $J_{11\beta,12\alpha} = 13.5$  Hz); H-11 $\beta$  and H-12 $\beta$  ( $J_{11\beta,12\beta} = 7.9$  Hz). Therefore, compound **1** was determined to be 11 $\alpha$ -hydroxy-7-deacetoxy-7-oxogedunin, which has been thus isolated in Nature for the first time.

**Figure 1.** Chemical structures for compounds **1–4**.

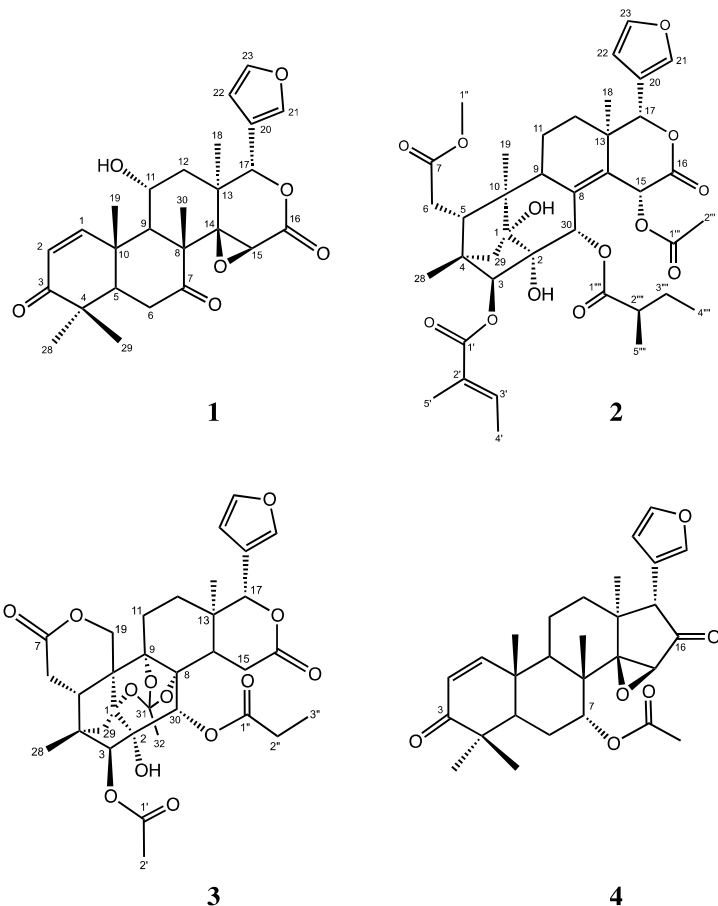


**Figure 2.** Key HMBC, COSY, and NOESY correlations for carapanolide J (**1**).

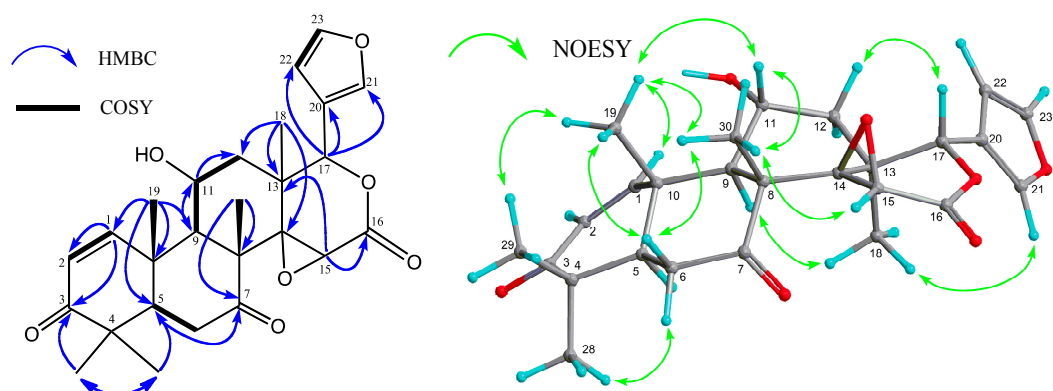


**Table 1.**  $^1\text{H}$  (600 MHz) and  $^{13}\text{C}$  (150 MHz) NMR spectroscopic data of compound **1**.

Position	<b>1</b>		<b>1</b>	$^1\text{H}^a$ ( $J$ , Hz)	$^{13}\text{C}^b$
	$^1\text{H}^a$ ( $J$ , Hz)	$^{13}\text{C}^b$			
1	8.24	d 10.3 (2)	160.2		
2	5.84	d 10.3 (1)	124.9		
3			203.0		
4			45.6		
5	2.21	dd 3.2 (6 $\alpha$ ), 14.6 (6 $\beta$ )	53.9		
6 $\alpha$	2.38	dd 3.2 (5), 13.8 (6 $\beta$ )	36.3		
6 $\beta$	2.93	dd 13.8 (6 $\alpha$ ), 14.6 (5)			120.0
7			207.7	7.44	m
8			53.4	6.39	dd 0.6 (21), 1.7 (23)
9	2.45	d 10.2 (11)	51.3	7.42	t 1.7 (21, 22)
10			40.9	1.17	s
11 $\beta$	4.47	ddd 7.9 (12 $\beta$ ), 10.2 (9), 13.5 (12 $\alpha$ )	67.3	1.16	s
12 $\alpha$	1.46	dd 13.5 (11), 13.8 (12 $\beta$ )	44.6	1.28	s
12 $\beta$	2.21	dd 7.9 (11), 13.8 (12 $\alpha$ )		11-OH	1.83
13			38.0		

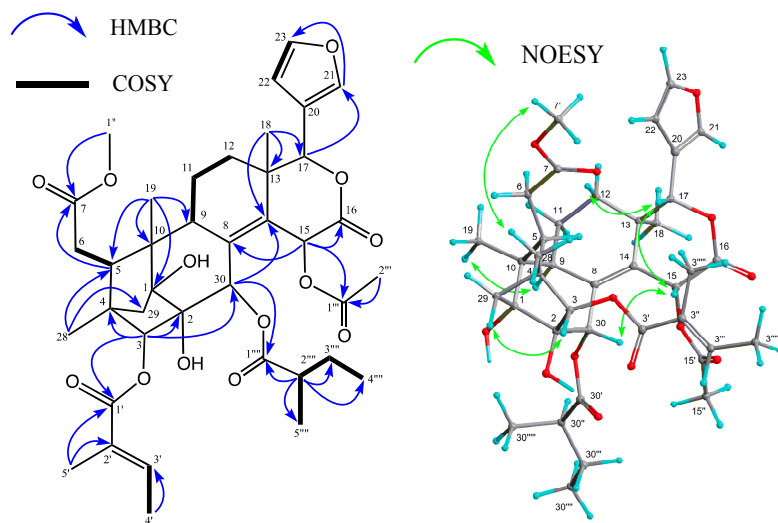
<sup>a</sup> Measured at 600 MHz in  $\text{CDCl}_3$ ; <sup>b</sup> Measured at 150 MHz in  $\text{CDCl}_3$ . Assignments are based on HMBC spectrum.

Carapanolide K (**2**), which was isolated as a colorless amorphous solid, had the molecular formula  $\text{C}_{39}\text{H}_{50}\text{O}_{13}$  ( $[\text{M} + \text{Na}]^+$ ;  $m/z$  749.3152, calcd. for 749.3155) as determined by HRFABMS. The IR spectrum showed the presence of a hydroxyl at  $\nu_{\text{max}}$   $3446\text{ cm}^{-1}$ , and ester groups at  $\nu_{\text{max}}$   $1766$ ,  $1735$ , and  $1698\text{ cm}^{-1}$ . The  $^1\text{H}$ - and  $^{13}\text{C}$ -NMR spectra (Table 2) indicated the presence of three methyls [ $\delta_{\text{H}}$  0.83, 1.09, 1.14 (each 3H, s)], an acetyl group [ $\delta_{\text{H}}$  2.07 (3H, s),  $\delta_{\text{C}}$  21.1 (q), 169.9 (s)], 2-methylbutanoyl group [ $\delta_{\text{H}}$  0.90 (3H, t), 1.13 (3H, d), 1.48 and 1.64 (each 1H, m), 2.38 (1H, m),  $\delta_{\text{C}}$  176.3 (s)], tigloyl group [ $\delta_{\text{H}}$  1.77 (3H, dd), 1.98 (3H, t), 7.14 (1H, qq);  $\delta_{\text{C}}$  168.5 (s)], methoxycarbonyl group [ $\delta_{\text{H}}$  3.72 (3H, s),  $\delta_{\text{C}}$  52.0 (q), 174.2 (s)],  $\delta$ -lactone [ $\delta_{\text{H}}$  5.36 (1H, s),  $\delta_{\text{C}}$  80.3 (d), 167.8 (s)], two tertiary hydroxyl groups [ $\delta_{\text{C}}$  77.0 (s), 83.6 (s)], a tetrasubstituted double bond [ $\delta_{\text{C}}$  134.9 (s), 135.4 (s)], and furan ring [ $\delta_{\text{H}}$  6.47 (dd), 7.41 (t), 7.58 (t)]. In the HMBC spectrum, cross-peaks were observed between Me-18 [ $\delta_{\text{H}}$  1.09 (s)] and C-12, C-13, C-14 [ $\delta_{\text{C}}$  135.4 (s)], and C-17 [ $\delta_{\text{C}}$  80.3 (d)]; between Me-19 [ $\delta_{\text{H}}$  1.14 (s)] and C-1 [ $\delta_{\text{C}}$  83.6 (s)], C-5, C-9, and C-10; between Me-28 [ $\delta_{\text{H}}$  0.83 (s)] and C-3 [ $\delta_{\text{C}}$  88.2 (d)], C-4, C-5, and C-29; between H-3 [ $\delta_{\text{H}}$  4.73 (s)] and C-1, C-2 [ $\delta_{\text{C}}$  77.0 (d)], C-4, C-5, C-28, C-29, C-30 [ $\delta_{\text{C}}$  69.7 (d)], and C-3' [ $\delta_{\text{C}}$  168.5 (s)]; between H-5 [ $\delta_{\text{H}}$  2.88 (dd)] and C-1, C-3, C-4, C-6, C-7 [ $\delta_{\text{C}}$  174.2 (s)], C-10, C-19, C-28, and C-29; between H-30 [ $\delta_{\text{H}}$  5.41 (s)] and C-1, C-2, C-3, C-8 [ $\delta_{\text{C}}$  134.9 (s)], C-9, and C-30' [ $\delta_{\text{C}}$  176.3 (s)]. The positions of the hydroxyl, 2-methylbutanoyl, methoxycarbonyl, and tigloyl groups were identified by detailed  $^1\text{H}$ - $^1\text{H}$  COSY and HMBC correlations (Figure 3). In addition, the cross peaks between H-9 and H-30, and C-8 [ $\delta_{\text{C}}$  134.9 (s)]; between H-30, H-15, and C-14 [ $\delta_{\text{C}}$  135.4 (s)] revealed that compound **2** was a phragmalin-8(14)-ene derivative [14]. In the NOESY spectrum, significant NOEs (Figure 3) were observed between H-3 [ $\delta_{\text{H}}$  4.73 (s)] and H-29 pro-S, H-30, and Me-28; between H-5 [ $\delta_{\text{H}}$  2.88 (dd)] and Me-28 and H-30; between Me-18 and H-11 $\alpha$  and H-12 $\alpha$ ; between Me-19 and H-11 $\alpha$ , between H-15 and H-17 $\beta$ , H-30, H-3', H-5', and H-2'''; therefore, the 2-methylbutanoyl group at C-30 and acetoxy group at C-15 were all  $\alpha$  while the tigloyl group at C-3 had a  $\beta$  orientation. The configuration

of the 2-methylbutanoyl group at C-30 was deduced to be *R* because the chemical shift value and NOESY correlation were very similar to that of carapanolide F [11], which was determined as 2*R* by single-crystal X-ray diffraction analysis.

Carapanolide L (**3**) was obtained as a colorless amorphous solid, and its molecular formula was established as C<sub>33</sub>H<sub>38</sub>O<sub>13</sub> ([M + H]<sup>+</sup>; *m/z* 643.2391, calcd. for 643.2391) by HRFABMS, implying 15 degrees of unsaturation. The IR spectrum showed the presence of a hydroxyl at  $\nu_{\text{max}}$  3352 cm<sup>-1</sup>, and ester groups at  $\nu_{\text{max}}$  1742 cm<sup>-1</sup>. The <sup>1</sup>H- and <sup>13</sup>C-NMR data indicated that eight of the 15 units of unsaturation came from two carbon–carbon double bonds and four ester carbonyls, including two lactone carbonyls. Therefore, the remaining degrees of unsaturation required **3** to be nonacyclic. The <sup>1</sup>H- and <sup>13</sup>C-NMR spectra of **3** (Table 2) indicated the presence of two tertiary methyls [ $\delta_{\text{H}}$  1.00, 1.13 (each s)], an acetyl [ $\delta_{\text{H}}$  2.19 (s);  $\delta_{\text{C}}$  21.6 (q), 170.4 (s)], propanoyl [ $\delta_{\text{H}}$  1.09 (3H, t), 2.36 (1H, dq), 2.39 (1H, dq);  $\delta_{\text{C}}$  8.6 (q), 27.8 (t), 172.8 (s)], and orthoacetyl group [ $\delta_{\text{H}}$  1.70 (s);  $\delta_{\text{C}}$  21.0 (q), 119.6 (s)], four methylenes, including an oxymethylene [ $\delta_{\text{H}}$  4.38 and 4.77 (each 1H, d), five *sp*<sup>3</sup> methines, including three oxymethines [ $\delta_{\text{H}}$  4.66 (s), 5.35 (s), and 5.71 (s)], a furan ring [ $\delta_{\text{H}}$  6.41 (dd), 7.44 (t), and 7.48 (m)], seven *sp*<sup>3</sup> quaternary carbons, including four oxycarbon [ $\delta_{\text{C}}$  79.5 (s), 85.4 (s), 86.3 (s), and 86.4 (s)], two ester carbonyls [ $\delta_{\text{C}}$  170.4, and 172.8 (each s)], and two lactone carbonyl [ $\delta_{\text{C}}$  169.8, and 171.1 (s)]. An analysis of the <sup>1</sup>H-<sup>1</sup>H COSY spectrum of **3** revealed the partial structures shown in bold face in Figure 4. In the HMBC spectrum (Figure 4), cross-peaks were observed from Me-18 [ $\delta_{\text{H}}$  1.13 (s)] to C-12, C-13, C-14, and C-17 ( $\delta_{\text{C}}$  78.4); from Me-28 [ $\delta_{\text{H}}$  1.00 (s)] to C-3, C-4, C-5, and C-29; from H-30 [ $\delta_{\text{H}}$  5.71 (s)] to C-1 [ $\delta_{\text{C}}$  85.4 (s)], C-2 [ $\delta_{\text{C}}$  79.5 (s)], C-3 [ $\delta_{\text{C}}$  83.9 (d)], C-8 [ $\delta_{\text{C}}$  86.4 (s)], and C-9 [ $\delta_{\text{C}}$  86.3 (s)] from H-14 [ $\delta_{\text{H}}$  1.00 (s)] to C-8, C-9, C-12, C-13, C-15, and C-16 [ $\delta_{\text{C}}$  169.8 (s)]. Therefore, the planar structure of **3** was established as phragmalin-1,8,9-orthoacetate [13], and the positions of the hydroxyl, acetyl, and *n*-propyl groups were located at C-2, C-3, and C-30 by detailed <sup>1</sup>H-<sup>1</sup>H COSY and HMBC correlations (Figure 3). In the NOESY spectrum, significant NOEs (Figure 3) were observed between H-3 [ $\delta_{\text{H}}$  4.73 (s)] and H-29 *pro-S*, H-30, and Me-28; between H-5 $\beta$  [ $\delta_{\text{H}}$  2.68 (dd)] and H-12 $\beta$ , Me-28, and H-30; between H-15 $\beta$  [ $\delta_{\text{H}}$  3.19 (dd)] and H-30; between H-17 $\beta$  [ $\delta_{\text{H}}$  5.35 (s)] and H-12 $\beta$ , H-15 $\beta$ , H-22, and H-30 $\beta$ , between Me-18 [ $\delta_{\text{H}}$  1.13 (s)] and H-11 $\alpha$ , H-12 $\alpha$  and Me-32. Therefore, the relative structure of **3** was established as shown in Figure 1.

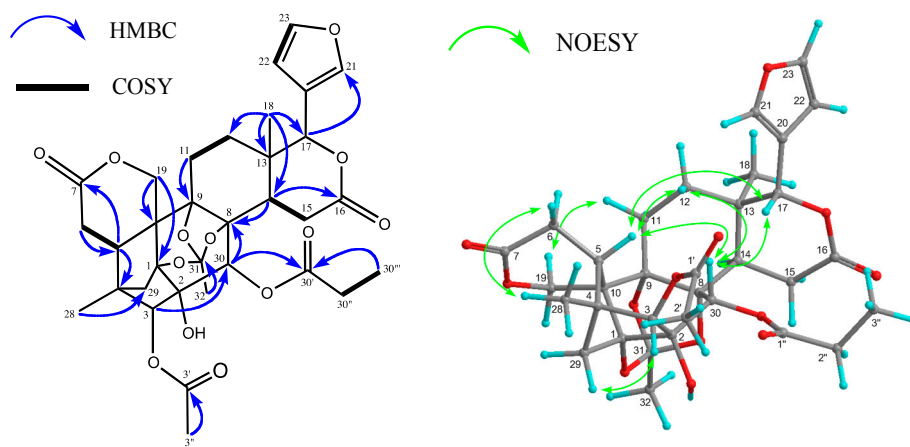
**Figure 3.** Selected  $^1\text{H}$ - $^1\text{H}$  COSY, HMBC and NOESY correlations for carapanolide K (2).



**Table 2.**  $^1\text{H}$ -NMR and  $^{13}\text{C}$ -NMR data for compounds **2** and **3**.

Position	2		3	
	$^1\text{H}^a$ ( $J$ , Hz)	$^{13}\text{C}^b$	$^1\text{H}^a$ ( $J$ , Hz)	$^{13}\text{C}^b$
1		83.6		85.4
2		77.0		79.5
3	4.73	s	88.2 4.66	83.9
4			43.1	45.2
5	2.88	dd 1.2 (6B), 5.3 (6A)	37.5 2.68	dd 3.5 (6B), 5.5 (6A)
6	A 2.32	d 5.3 (5)	33.7 2.46	dd 5.5 (5), 17.6 (6B)
	B 2.33	d 1.2 (5)	2.66	dd 3.5 (5), 17.6 (6A)
7			174.2	171.1
8			134.9	86.4
9	2.73	d 7.7	35.9	86.3
10			47.5	44.7
11	$\alpha$ 1.70	m	18.3 1.85	dt 2.9 (11 $\alpha$ ), 14.7 (12 $\alpha,\beta$ )
	$\beta$ 1.89	m	2.27	m
12	$\alpha$ 1.05	m	28.5 1.48	m
	$\beta$ 1.40	dt 3.2 (12 $\alpha$ ), 14.1 (11 $\beta$ )	1.38	m
13			38.9	34.5
14			135.4 2.02	dd 2.0 (15 $\beta$ ), 10.5 (15 $\alpha$ )
15	$\alpha$ 6.28	d 2.4	64.2 3.19	dd 10.5 (14), 20.0 (15 $\beta$ )
	$\beta$			dd 2.0 (14), 20.0 (15 $\alpha$ )
16			167.8	169.8
17	5.36	s	80.3 5.35	s
18	1.09	s	16.7 1.13	s
19	$\alpha$ 1.14	3H, s	17.3 4.77	d 13.8 (19 $\beta$ )
	$\beta$		4.38	d 13.8 (19 $\alpha$ )
20			120.5	120.8
21	7.58	t 0.8 (22)	142.0 7.48	t 0.8 (22)
22	6.47	dd 0.8 (21), 1.6 (23)	109.9 6.41	dd 0.8 (21), 1.8 (23)
23	7.41	t 1.6 (22)	143.0 7.44	t 1.8 (22)
28	0.83	s	14.8 1.00	s
29	<i>pro-R</i> 1.58	d 11.0 (29 <i>pro-S</i> )	39.8 1.80	d 11.1 (29 <i>pro-S</i> )
	<i>pro-S</i> 1.86	d 11.0 (29 <i>pro-R</i> )	2.25	d 11.1 (29 <i>pro-R</i> )
30	5.41	s	69.7 5.71	s
31				70.0
32			1.70	119.6
1'			168.5	21.0
2'			130.0 2.19	170.4
3'	7.14	qq 7.0 (4'), 1.1 (5')	12.2	21.6
4'	1.77	dd 1.1 (5'), 7.0 (3')	139.2	
5'	1.98	t 1.1 (3', 4')	14.5	
1"	3.72	s	52.0	172.8
2"	A		2.36	dq 7.5 (3"), 9.7 (2"B)
	B		2.39	dq 7.5 (3"), 9.7 (2"A)
3"			1.09	3H, t 7.5 (2"A, 2"B)
1'''			169.9	8.6
2'''	2.07	s	21.1	
1''''			176.3	
2''''	A 2.38	m	40.9	
	B			
3''''	A 1.48	m	26.5	
	B 1.64	m		
4''''	0.90	t 7.3 (3'''A, 3'''B)	16.4	
5''''	1.13	d 7.0 (2'''")	11.3	

<sup>a</sup> Measured at 600 MHz in  $\text{CDCl}_3$ ; <sup>b</sup> Measured at 150 MHz in  $\text{CDCl}_3$ . Assignments are based on HMBC spectrum.

**Figure 4.** Key HMBC,  $^1\text{H}$ — $^1\text{H}$  COSY, and NOESY correlations of carapanolide L (3).

Physiological nitric oxide (NO) is involved in blood pressure regulation and blood flow distribution, whereas its overexpression may induce tissue injury, multiple organ dysfunction, and death, as well as systemic inflammatory responses in sepsis, such as hypotension, cardiodepression, and vascular hyporeactivity [15]. In the present study, four limonoids and L-NMMA, an inducible nitric oxide synthase (iNOS) inhibitor, were evaluated for their inhibitory effects on NO production in LPS-stimulated RAW264.7 cells (Table 3). To determine safe concentrations, the cytotoxicities of these limonoids against RAW 264.7 were assessed by the MTT assay. Compounds **1** and **3** showed non-toxicities at 3–100  $\mu\text{M}$ , whereas **4** and **2** exhibited moderate cytotoxicities ( $\text{IC}_{50}$  **4**: 21.3  $\mu\text{M}$ ; **2**: 15.2  $\mu\text{M}$ ). In the inhibitory assay of NO production, compound **1** showed similar inhibitory activities (produced NO 83.4% at 10  $\mu\text{M}$ ; 61.8% at 30  $\mu\text{M}$ ; 16.8% at 100  $\mu\text{M}$ ) to the positive control, L-NMMA (produced NO 79.3% at 10  $\mu\text{M}$ ; 58.2% at 30  $\mu\text{M}$ ; 39.9% at 100  $\mu\text{M}$ ), with no cytotoxicities. Compound **4** exhibited superior inhibitory activities on NO production at non-toxic concentrations (produced NO 74.0% at 3  $\mu\text{M}$ ; 30.0% at 10  $\mu\text{M}$ ) to those of L-NMMA. These results suggested that compound **1** may be valuable as potential inhibitors of NO production.

**Table 3.** Inhibitory effects of NO production by limonoids from the seeds of *Carapa guianensis*.

Compound	Concentration ( $\mu\text{M}$ )				
	3	10	30	100	$\text{IC}_{50}$ ( $\mu\text{M}$ )
<b>1</b>	Produced NO (%) <sup>a</sup>	92.1 $\pm$ 1.5	83.4 $\pm$ 3.1	61.8 $\pm$ 1.8	16.8 $\pm$ 0.0
	Cell viability (%) <sup>a</sup>	102.4 $\pm$ 0.8	101.0 $\pm$ 1.7	102.8 $\pm$ 0.6	103.4 $\pm$ 1.8
<b>2</b>	Produced NO (%)	78.6 $\pm$ 1.9	58.3 $\pm$ 2.8	25.8 $\pm$ 7.0	7.1 $\pm$ 1.2
	Cell viability (%)	81.4 $\pm$ 0.8	65.6 $\pm$ 0.2	33.6 $\pm$ 6.3	0.4 $\pm$ 0.4
<b>3</b>	Produced NO (%)	95.6 $\pm$ 2.5	95.4 $\pm$ 1.2	95.4 $\pm$ 2.9	78.4 $\pm$ 2.3
	Cell viability (%)	97.6 $\pm$ 0.6	97.3 $\pm$ 1.3	100.5 $\pm$ 0.4	94.4 $\pm$ 1.0
<b>4</b>	Produced NO (%)	74.0 $\pm$ 5.0	30.0 $\pm$ 2.3	7.5 $\pm$ 1.0	3.9 $\pm$ 1.8
	Cell viability (%)	93.6 $\pm$ 1.4	99.7 $\pm$ 0.8	6.8 $\pm$ 0.3	3.3 $\pm$ 0.3
L-NMMA <sup>b</sup>	Produced NO (%)	93.0 $\pm$ 3.3	79.3 $\pm$ 0.8	58.2 $\pm$ 2.4	39.9 $\pm$ 1.7
	Cell viability (%)	103.5 $\pm$ 0.5	102.0 $\pm$ 1.5	94.1 $\pm$ 1.4	96.5 $\pm$ 2.5

<sup>a</sup> Produced NO (%) and cell viability (%) were determined based on the absorbance at 570 nm, respectively, by comparison with values for DMSO (100%). Each value represents the mean  $\pm$  standard error (S.E.) of three determinations. The concentration of DMSO in the sample solution was 2  $\mu\text{L}/\text{mL}$ ; <sup>b</sup> Positive control.

### 3. Experimental Section

#### 3.1. General Procedures

Melting points were determined on a Yanagimoto micro-melting point apparatus and were uncorrected. Optical rotations were measured using a JASCO DIP-1000 digital polarimeter. IR spectra were recorded using a Perkin-Elmer 1720X FTIR spectrophotometer. <sup>1</sup>H- and <sup>13</sup>C-NMR spectra were obtained on an Agilent vnmrs 600 spectrometer with standard pulse sequences, operating at 600 and 150 MHz, respectively. CDCl<sub>3</sub> was used as the solvent and TMS, as the internal standard. FABMS were recorded on a JEOL-7000 mass spectrometer. Column chromatography was carried out over silica gel (70–230 mesh, Merck, Darmstadt, Germany) and MPLC was carried out with silica gel (230–400 mesh, Merck). HPLC was run on a JASCO PU-1586 instrument equipped with a differential refractometer (RI 1531). Fractions obtained from column chromatography were monitored by TLC (silica gel 60 F<sub>254</sub>, Merck).

#### 3.2. Plant Material

The oil of (2.03 kg) *Carapa guianensis* AUBLET (Meliaceae) was collected in the Amazon, Brazil, in March 2013. Kindly provided by Mr. Akira Yoshino (who is a representative of the NGO “Green Heart Love Amazon Project”). A voucher specimen (CGS-01-2) was deposited in the Herbarium of the Laboratory of Medicinal Chemistry, Osaka University of Pharmaceutical Sciences.

#### 3.3. Isolation of Compounds 1–4

The seed oil of *Carapa guianensis* AUBLET (Meliaceae) (2.03 kg) was dissolved in CHCl<sub>3</sub> (1 L) and the CHCl<sub>3</sub> solution was subjected to CC (silica gel 14 kg), to afford seven fractions: Fraction A (Fr. No. 1–85, 1.512 kg) was eluted with *n*-hexane-CHCl<sub>3</sub> = 1:1, B (Fr. No. 86–179, 229.1 g) was eluted with CHCl<sub>3</sub>, C (Fr. No. 180–220, 29.3 g) was eluted with CHCl<sub>3</sub>-EtOAc = 5:1, D (Fr. No. 221–225, 13.2 g) was eluted with CHCl<sub>3</sub>-EtOAc = 2:1, E (Fr. No. 226–265, 84.5 g) was eluted with CHCl<sub>3</sub>-EtOAc = 2:1, F (Fr. No. 266–290, 25.3 g) was eluted with EtOAc, G (Fr. No. 291–315, 72.8 g) was eluted with EtOAc:MeOH = 5:1, and H (Fr. No. 316–333, 45.4 g) was eluted with MeOH. Residue D was rechromatographed over a silica gel column (CC) (230–400 mesh, 300 g) eluted with *n*-hexane- EtOAc (1:1) to give 13 fractions: D1 (Fr. No. 1–35, 1.52 g), D2 (Fr. No. 36–49, 0.81 g), D(3) (Fr. No. 50–88, 0.70 g), D(4) (Fr. No. 89–115, 0.53 g), D(5) (Fr. No. 116–130, 0.60 g), D(6) (Fr. No. 131–140, 0.52 g), D(7) (Fr. No. 141–205, 0.47 g), D(8) (Fr. No. 206–215, 0.51 g), D(9) (Fr. No. 216–220, 0.42 g), D(10) (Fr. No. 221–240, 0.40 g), D(11) (Fr. No. 241–250, 1.11 g), and D(12) (Fr. No. 251–313, 1.36 g). Fraction D(6) was subjected to CC (230–400 mesh, 40 g) eluted with *n*-hexane-EtOAc (3:1) to give an amorphous solid (24.1 mg) that was separated by HPLC (ODS, 75% MeOH, at 25 °C, flow rate 4.0 mL·min<sup>−1</sup>, UV = 220 nm, column 250 × 20 mm i.d., 5 µm) to give compounds **2** (6.2 mg) and **3** (1.79 mg). Fraction D(8) was subjected to CC (230–400 mesh, 40 g) eluted with *n*-hexane-EtOAc (3:1) to give an amorphous solid (34.0 mg) that was subjected to CC (230–400 mesh, 40 g) eluted with *n*-hexane-EtOAc (3:1) to give an amorphous solid that was purified by HPLC (ODS, 75% MeOH, at 25 °C, flow rate 4.0 mL·min<sup>−1</sup>, UV = 220 nm, column 250 × 20 mm i.d., 5 µm) to give compounds **1** (7.5 mg) and **4** (3.8 mg). Fraction D(9) was subjected to CC (230–400 mesh, 30 g) eluted with

*n*-hexane–EtOAc (3:1) to give an amorphous solid (25.5 mg) that was separated by HPLC (ODS, 70% MeOH, at 25 °C, flow rate 4.0 mL·min<sup>-1</sup>, UV = 220 nm, column 250 × 20 mm i.d., 5 µm) to give compound **3** (6.2 mg).

### 3.4. Analytical Data

Compound **1**. Colorless crystals; mp 172–174 °C (from MeOH-CHCl<sub>3</sub>); [α]<sub>D</sub><sup>26</sup> −18.7° (c 0.1, CHCl<sub>3</sub>); HRFABMS *m/z*: 455.2075 [M+H]<sup>+</sup> (C<sub>26</sub>H<sub>31</sub>O<sub>7</sub>, calcd for 455.2080); UV (EtOH) λ<sub>max</sub> nm (log ε): 230 (3.85), 237 (3.80), 248 (3.63); IR (KBr) ν<sub>max</sub> cm<sup>−1</sup>; 3503 (OH), 2926, 1727 (O-C=O), 1671 (C=C-C=O); <sup>1</sup>H- and <sup>13</sup>C-NMR, see Table 1. FABMS *m/z* (rel. int.): 477 ([M+Na]<sup>+</sup>, 15), 455 ([M+H]<sup>+</sup>, 71), 83 (100).

Compound **2**. Colorless amorphous solids; [α]<sub>D</sub><sup>26</sup> −72.2° (c 0.1, CHCl<sub>3</sub>); HRFABMS *m/z*: 749.3152 [M+Na]<sup>+</sup> (C<sub>39</sub>H<sub>50</sub>O<sub>13</sub>Na, calcd for 749.3155); UV λ<sub>max</sub> (EtOH) nm (log ε): 227 (4.19), 304 (3.98), 315 (4.00), 334 (3.72); IR (KBr) ν<sub>max</sub> cm<sup>−1</sup>: 3446 (OH), 2967, 1766 and 1735, 1698; <sup>1</sup>H- and <sup>13</sup>C-NMR, see Table 2. FABMS *m/z* (rel. int.): 749 (33) ([M+Na]<sup>+</sup>, 3), 727 ([M+H]<sup>+</sup>, 100).

Compound **3**. Colorless amorphous solids; [α]<sub>D</sub><sup>26</sup> −46.8° (c 0.1, CHCl<sub>3</sub>); HRFABMS *m/z*: 643.2391 [M+H]<sup>+</sup> (C<sub>33</sub>H<sub>38</sub>O<sub>13</sub>, calcd for 643.2391); UV λ<sub>max</sub> (EtOH) nm (log ε): 208 (1.26), IR (KBr) ν<sub>max</sub> cm<sup>−1</sup>: 3352 (OH), 1742 (O-C=O); <sup>1</sup>H- and <sup>13</sup>C-NMR, see Table 2. FABMS *m/z* (rel. int.): 665 (33) ([M+Na]<sup>+</sup>, 12), 643 ([M+H]<sup>+</sup>, 100).

### 3.5. Determination of RAW264.7 Cell Proliferation

RAW264.7 cell proliferation was examined according to a method reported previously [16] with some modifications. Briefly, RAW264.7 cells (5 × 10<sup>4</sup> cells in 100 µL) were seeded onto 96-well microplates, and incubated for 24 h. D-MEM (100 µL) containing test samples (final concentration of 100, 30, 10, or 3 µM) dissolved in DMSO (final concentration 0.2%) was added. After the cells had been treated for 24 h, the MTT solution was added. After 3 h of incubation, 20% sodium dodecyl sulfate (SDS) in 0.1 M HCl was added to dissolve the formazan produced by the cells. The absorbance of each well was read at 570 nm using a microplate reader. The optical density of vehicle control cells was assumed to be 100%.

### 3.6. Inhibitory Assay of NO Production

An inhibitory assay of nitric oxide production was performed according to a method reported previously [17] with slight modifications. Briefly, RAW264.7 cells (5 × 10<sup>4</sup> cells in 100 µL) were seeded onto 96-well microplates, and incubated for 24h. D-MEM (100 µL) containing test samples (final concentration of 100, 30, 10, or 3 µM) dissolved in DMSO (final concentration 0.2%) and LPS (final concentration of 5 µg/mL) were added. After cells had been treated for 24 h, 50 µL of 0.1% *N*-(1-naphtyl)ethylenediamine in H<sub>2</sub>O and 50 µL of 1% sulfanylamide in 5% phosphoric acid were added. After being incubated for 30 min, the absorbance of each well was read at 570 nm using a microplate reader. The optical density of vehicle control cells was assumed to be 100%.

#### 4. Conclusions

A novel gedunin and two novel phragmalin-type limonoids, named carapanolides J–L (compounds **1–3**), as well as a known gedunin-type limonoid **4** were isolated from the seeds of *Carapa guianensis* (andiroba). Their structures were determined by spectroscopic analyses. Compound **1** showed similar inhibitory activities (produced NO 83.4% at 10  $\mu$ M; 61.8% at 30  $\mu$ M; 16.8% at 100  $\mu$ M) to positive control, L-NMMA (produced NO 79.3% at 10  $\mu$ M; 58.2% at 30  $\mu$ M; 39.9% at 100  $\mu$ M), with no cytotoxicity. Known compound **4** exhibited superior inhibitory NO production activities at non-toxic concentrations (produced NO 74.0% at 3  $\mu$ M; 30.0% at 10  $\mu$ M) to those of L-NMMA. These results suggest that compound **1** may be a valuable potential inhibitor of NO production.

#### Acknowledgments

We thank Katsuhiko Minoura and Mihoyo Fujitake (this university) for the NMR and MS measurements.

#### Author Contributions

Y. Matsui and T. Inoue performed the isolation and structure elucidation. T. Kikuchi contributed to evaluation of bioactivities. T. Yamada, O. Muraoka and R. Tanaka prepared the manuscript and supervised whole research project.

#### Conflicts of Interest

The authors declare no conflict of interest.

#### References

1. Tan, Q.G.; Luo, X.D. Meliaceous limonoids: chemistry and biological activities. *Chem. Rev.* **2011**, *111*, 7437–7522.
2. Prophiro, J.S.; da Silva Mario, A.N.; Kanis, L.A.; da Rocha, L.C.B.P.; Duque-Luna, J.E.; da Silva, O.S. First report on susceptibility of wild *Aedes aegypti* (Diptera: Culicidae) using *Carapa guianensis* (Meliaceae) and *Copaifera* sp. (Leguminosae). *Parasitol. Res.* **2012**, *110*, 7699–7705.
3. Penido, C.; Costa, K.A.; Pennaforte, R.J.; Costa, M.F.S.; Pereira, J.F.G.; Siani, A.C.; Henriques, M.G.M.O. Anti-allergic effects of natural tetrnortriterpenoids isolated from *Carapa guianensis* Aublet on allergen-induced vascular permeability and hyperalgesia. *Inflamm. Res.* **2005**, *54*, 295–303.
4. Bickii, J.; Njifutie, N.; Foyere, J.A.; Basco, L.K.; Ringwald, P.J. *In vitro* antimalarial activity of limonoids from *Khaya grandifoliola* C.D.C. (Meliaceae). *J. Ethnopharmacol.* **2000**, *69*, 27–33.
5. Penido, C.; Conte, F.P.; Chagas, M.S.S.; Rodrigue, C.A.B.; Pereira, J.F.G.; Henriques, M.G.M.O. Antiinflammatory effects of natural tetrnortriterpenoids isolated from *Carapa guianensis* Aublet on zymosan-induced arthritis in mice. *Inflamm. Res.* **2006**, *55*, 457–464.

6. Ferraris Fausto, K.; Rodrigues, R.; da Silva, V.P.; Figueiredo, R.; Penido, C.; Henriques, M.G.M.O. Modulation of T lymphocyte and eosinophil functions *in vitro* by natural tetranoltriterpenoids isolated from *Carapa guianensis* Aublet. *Int. Immunopharmacol.* **2011**, *11*, 1–11.
7. Miranda Junior, R.N.C.; Dolabela, M.F.; da Silva, M.N.; Povoa, M.M.; Maia, J.G.S. Antiplasmoidal activity of the andiroba (*Carapa guianensis* Aublet., Meliaceae) oil and its limonoid-rich fraction. *J. Ethnopharmacol.* **2012**, *142*, 679–683.
8. Costa-Silva, H.; Lima, C.R.; Silva, E.J.R.; Araujo, A.V.; Fraga, M.C.C.R.; Ribeiro, E.; Ribwiros, A.; Arruda, A.C.; Lafayette, S.S.L.; Wanderley, J. Acute and subacute toxicity of the *Carapa guianensis* Aublet (Meliaceae) seed oil. *J. Ethnopharmacol.* **2008**, *116*, 495–500.
9. Inoue, T.; Nagai, Y.; Mitooka, A.; Ujike, R.; Muraoka, O.; Yamada, T.; Tanaka, R. Carapanolides A and B: unusual 9,10-seco-mexicanolides having a 2R,9S-oxygen bridge from the seeds of *Carapa guianensis*. *Tetrahedron Lett.* **2012**, *53*, 6685–6688.
10. Inoue, T.; Matsui, Y.; Kikuchi, T.; In, Y.; Yamada, T.; Muraoka, O.; Matsunaga, S.; Tanaka, R. Guianolides A and B, New Carbon Skeletal Limonoids from the seeds of *Carapa guianensis*. *Org. Lett.* **2013**, *15*, 3018–3021.
11. Inoue, T.; Matsui, Y.; Kikuchi, T.; In, Y.; Muraoka, O.; Yamada, T.; Tanaka, R. Carapanolides C–I from the seeds of andiroba (*Carapa guianensis*, Meliaceae). *Fitoterapia* **2014**, *96*, 56–64.
12. Malathi, R.; Rajan, S.S.; Mohan Kumar, R.; Narasimhan, S.; Ravikumar, K. Epoxyazadiradione. *Acta Crystallogr.* **2007**, *E63*, 2483–2485.
13. Tanaka, Y.; Yamada, T.; In, Y.; Muraoka, O.; Kajimoto, T.; Tanaka, R. Absolute stereostructure of Andriolides A–G from the flower of *Carapa guianensis* (Meliaceae). *Tetrahedron* **2011**, *67*, 782–792.
14. Ravangpai, W.; Sommit, D.; Teerawatananond, T.; Sinpranee, N.; Palaga, T.; Pengpreecha, S.; Muangsin, N.; Pudhom, K. Limonoids from seeds of Thai *Xylocarpus moluccensis*. *Bioorg. Med. Chem. Lett.* **2011**, *21*, 4485–4489.
15. Kirkeboen, K.A.; Strand, O.A. The role of nitric oxide in sepsis—an overview. *Acta Anaesthesiol. Scand.* **1999**, *43*, 275–288.
16. Yamada, T.; Muroga, Y.; Jinno, M.; Kajimoto, T.; Usami, Y.; Numata, A.; Tanaka, R. New class azaphilone produced by a marine fish-derived *Chaetomium globosum*. The stereochemistry and biological activities. *Bioorg. Med. Chem.* **2011**, *19*, 4106–4113.
17. Yamasaki, F.; Machida, S.; Nakata, A.; Nugroho, A.E.; Hirasawa, Y.; Kaneda, T.; Morita, H. Haworforbins A–C, new phenolics from *Haworthia cymbiformis*. *J. Nat. Med.* **2013**, *67*, 212–216.

*Sample Availability:* Not available.